HHS Public Access

Author manuscript

Hippocampus. Author manuscript; available in PMC 2018 March 19.

Published in final edited form as:

Hippocampus. 2017 February ; 27(2): 169–183. doi:10.1002/hipo.22681.

Repetition reveals ups and downs of hippocampal, thalamic, and neocortical engagement during mnemonic decisions

Zachariah M. Reagh[1,*], **Elizabeth A. Murray**[1], and **Michael A. Yassa**[1,*]

[1]Department of Neurobiology and Behavior and the Center for the Neurobiology of Learning and Memory; University of California, Irvine, Irvine, CA

Abstract

The extent to which current information is consistent with past experiences and our capacity to recognize or discriminate accordingly are key factors in flexible memory-guided behavior. Despite a wealth of evidence linking hippocampal and neocortical computations to these phenomena, many important factors remain poorly understood. One such factor is repeated encoding of learned information. In this experiment, participants completed a task in which study stimuli were incidentally encoded either once or three separate times during high-resolution fMRI scanning. We asked how repetition influenced recognition and discrimination memory judgments, and how this affects engagement of hippocampal and neocortical regions. Repetition revealed shifts in engagement in an anterior (ventral) CA1-thalamic-medial prefrontal network related to true and false recognition. Conversely, repetition revealed shifts in a posterior (dorsal) dentate/CA3-parahippocampal-restrosplenial network related to accurate discrimination. These differences in engagement were accompanied by task-related correlations in respective anterior and posterior networks. In particular, the anterior thalamic region observed during recognition judgments is functionally and anatomically consistent with nucleus reuniens in humans, and was found to mediate correlations between the anterior CA1 and medial prefrontal cortex. These findings offer new insights into how repeated experience affects memory and its neural substrates in hippocampal-neocortical networks.

Introduction

The mechanisms underlying the encoding and storage of memories are the subject of examination both in neurobiology and cognitive science. Despite decades of progress, many factors governing this process remain poorly understood. One such factor with a great deal of practical relevance is repeated encounters with the same information. Repetitive encoding often enhances one's ability to recognize studied stimuli (Ebbinghaus, 1913; Hintzman, 1976), which may be due to the similarity of neural activity gradually increasing with repeated exposures (Xue et al., 2010). However, beyond simple recognition (endorsing studied items as old), recent work from our lab suggests that multiple encounters with a studied stimulus may paradoxically hinder one's ability to discriminate that stimulus from

[*]Corresponding Authors: Z.M. Reagh and M.A. Yassa, 213 Qureshey Research Laboratory, Irvine, CA 92697-3800, Tel: (949) 824-1687, zreagh@uci.edu, myassa@uci.edu.

similar items in memory (Reagh & Yassa, 2014). The mechanism of such a trade off is presently unknown.

Studies of amnesic patients (Scoville & Milner, 1957; Reed & Squire, 1998) and experimental manipulations in animal models (Wang et al. 2009; Ross & Eichenbaum, 2006; Quinn et al., 2008) have demonstrated that the regions supporting memory encoding and storage may shift over time, a process that has been termed systems consolidation (McGaugh, 2000). The hippocampus is critical for the initial formation and storage of new memories, whereas many have argued that information is gradually stabilized over time for more permanent storage in the cerebral cortex (Dudai, 2004; McGaugh, 2000; Winocur & Moscovitch, 2011; Nadel et al., 2012; Meeter & Murre, 2004). This is often framed as a shift from hippocampus-dependent episodic memory to cortex-dependent semantic memory (Binder & Desai, 2011). These ideas form the neurobiological instantiation of the Complementary Learning Systems (CLS) computational model (McClelland, McNaughton, & O'Reilly, 1995), which has received much empirical support (Norman, 2010; O'Reilly et al., 2014). If repeated encoding stabilizes memory representations in the brain, this might, under some conditions, invoke mechanisms of hippocampal-neocortical communication.

It is widely theorized that the hippocampus acts as an index for the neocortex (Teyler & Discenna, 1986; Teyler & Rudy, 2007), but the nature of this communication is unresolved. Studies have observed during mnemonic tasks and at rest that activity in anterior and posterior hippocampal regions correlated with activity in anterior and posterior cortical areas respectively (Libby et al., 2012; Wang et al., *in press*), reflective of differences in structural connectivity (Aggleton, 2011). Recently, a view has emerged that the posterior hippocampus and associated cortical areas support fine-grained, specific, detailed information in memory, whereas the anterior hippocampus and cortices support coarse-grained, gist information that may generalize across experiences (Poppenk et al., 2013; Strange et al., 2014; Ritchey, Libby, & Ranganath, 2015). A possible implication is that highly detailed ‘pattern separated’ memories are more likely to be processed by the posterior hippocampus, while more generalized ‘pattern completed’ associations are more likely to be processed by the anterior hippocampus (Schlichting, Mumford, & Preston, 2015). Guided by this work, we hypothesized that the discrepancy we previously observed between enhanced recognition and lesser discrimination with repeated study (Reagh & Yassa, 2014) may involve repetition-related shifts in anterior versus posterior hippocampal-cortical networks.

We tested this hypothesis using a task designed to assess recognition and discrimination under conditions of single versus multiple study, along with high-resolution fMRI focused on the medial temporal lobes (MTL), anterior prefrontal cortices including perirhinal cortex (PRC), anterior cingulate cortex (ACC) and ventromedial prefrontal cortex (vmPFC), and posterior cortices including the parahippocampal cortex (PHC) and restrosplenial cortex (RSC). In addition to hippocampal and cortical regions of interest (ROIs), we additionally considered thalamic nucleus reuniens (NR), which is thought to provide a critical means of synchrony and information transfer between the prefrontal cortex and the hippocampus (Varela et al., 2014; Vertes et al., 2007; Griffin, 2015). Recent evidence has suggested that hippocampal-prefrontal communication is critical for learning and memory (Gonzalez et al., 2013; Goshen et al., 2011) and may be mediated by NR in the context of fear generalization

(Xu & Sudhof, 2013) as well as spatial navigation (Ito et al., 2015). However, little if any evidence exists pertaining to human NR. To examine the role of human thalamic NR in hippocampal-cortical communication, we used anatomical atlases to define an additional medial thalamic ROI centered on NR. We hypothesized that NR would mediate the functional connectivity between anterior hippocampus and ACC/vmPFC during recognition.

Materials and Methods

Participants

Twenty-one participants were recruited from the University of California, Irvine and surrounding Orange County community. Participants were right-handed adults between 18 and 27 years of age (mean = 21.3, SD = 1.8), and were screened for neurological and psychiatric disorders. Two participants were excluded due to excessive motion in the MRI scanner (>3mm displacement at any point in the experiment), one was excluded due to illness during participation, and one was excluded due to a software malfunction during scanning. The remaining 17 participants (9 female, age = 22.4, SD = 2.2) were included in analyses. Though we did not do formal power analyses prior to acquiring these data, this is considered to be a reasonable sample size for functional MRI studies using an *a priori* region of interest (ROI) based approach (Zandbelt et al., 2008). Participants gave written informed consent in accordance with the Institutional Review Board of the University of California, Irvine, and received monetary compensation for their participation.

Behavioral task and analysis

A schematic of the task can be viewed in Figure 1a. The experiment was conducted exactly the same as in our prior work (Reagh & Yassa, 2014). During the encoding phase of the experiment, participant viewed pictures of 300 common objects (e.g., an apple or a bicycle) presented in the center of the screen against a white background. Participants made incidental (non-mnemonic) judgments of whether each object was more commonly found “indoors” or “outdoors.” Responses were made via button presses on an MRI-compatible fiber-optic device. Of these images, half were viewed only once (1Enc) and half were viewed three times (3Enc), randomly interspersed throughout the entire encoding session, making for a total of 600 trials.

During the test phase, participants were presented with another series of 400 objects appearing at the center of the screen. Of these 400, 100 objects were exact repetitions (targets), 100 were entirely novel (foils), and 200 were similar but not identical to items previously studied (lures). Targets and lures corresponded to the original 300 objects. Half of the targets and half of the lures were based on studied items that were shown once, and half were based on studied items that were shown three times. Any given item from encoding was featured as either a target or a lure at test, but never both. Judgments consisted of simple “same” or “different” choices with respect to each test object, where a response of “same” to a target indicates successful recognition and a response of “different” to a lure indicates successful discrimination (conversely, a response of “same” to a lure is a false alarm). All images were viewed for 2.5 seconds, with a 0.5 second inter-stimulus interval.

We conducted pairwise comparisons between 1 vs. 3 conditions for target hits. We used two-tailed paired t-tests, and results of $p < 0.05$ two-tailed were reported as significant. For lure correct rejections, we analyzed data across similarity bins via a 2×5 (repetition by similarity) repeated measures ANOVA. Post hoc pairwise comparisons were carried out via the Holm-Šidák method, which controls the familywise error rate over t-tests in a sequentially rejective manner (Holm, 1979; Abdi, 2007). The Šidák correction is highly similar in both principle and outcome to the more common Bonferroni correction, but is considered to be more powerful (i.e., less pessimistic; see Abdi, 2007). Additionally, the Holm procedure adjusts significance at each comparison via ranking significance values and stepping down stringency with each evaluation (Holm, 1979). Post hoc contrasts are reported as significant if they pass this corrected threshold (reported as $p < 0.05$ corrected). For a summary of the lure rejection data, we calculated area under the curve (AUC) for each participant to capture their performance across all lure bins in a single summary measure. This was calculated as the summed averages of each similarity level added to the prior level such that the 'curve' being described is the relative gain in discrimination performance as lure similarity decreases. AUC values for 1Enc and 3Enc trials were compared via a simple paired t-test.

Decision criterion was calculated as z(Target Hit Rate) – z(Novel Foil False Alarm Rate) for targets, and z(Lure Rejection Rate) – z(Novel Foil False Alarm Rate) for lures. We used both the the 1Enc or 3Enc hit and rejection rates and compared between these conditions. We assessed differences between 1Enc and 3Enc criteria across targets and lures with t-tests, and took the numerical difference between these criteria to be used as covariates in ANCOVAs over regional response profiles in the fMRI analyses. Thus, significant main effects and interactions exist beyond any variance explained by differences in criterion across participants.

MRI data acquisition

Neuroimaging data were acquired on a 3.0 Tesla Philips Achieva scanner, using a 32-channel sensitivity encoding (SENSE) coil at the Neuroscience Imaging Center at the University of California, Irvine. A high-resolution 3D magnetization-prepared rapid gradient echo (MP-RAGE) structural scan (0.75 mm isotropic voxels) was acquired at the beginning of each session and used for co-registration. Functional MRI scans consisted of a T2*-weighted echo planar imaging (EPI) sequence using blood-oxygenation-level-dependent (BOLD) contrast: repetition time (TR)=2500 ms, echo time (TE)=26 ms, flip angle=70 degrees, 40 slices, 104 dynamics per run, 1.8 × 1.8 mm in plane resolution, 1.8 mm slice thickness with a 0.2 mm gap, field of view (FOV)=180×77.4×180. Slices were acquired as a partial axial volume and without offset or angulation (Fig. S4). Four initial "dummy scans" were acquired to ensure T1 signal stabilization. A total of 10 functional runs were acquired for each participant, 6 for the encoding phase and 4 for the test phase. Each functional run lasted 4 minutes and 30 seconds. For each subject, resting state EPI scans were acquired with the same parameters as the aforementioned task-acquired volumes.

MRI data preprocessing

All neuroimaging data were preprocessed and analyzed using Analysis of Functional NeuroImages (AFNI) (Cox, 1996) on GNU/Linux and Mac OSX platforms. Analyses

largely took place in accordance with the standardized afni_proc.py pipeline. Specifically, data were corrected for motion (3dvolreg) and slice timing shifts (3dTshift), masked to exclude voxels outside the brain (3dautomask), and were smoothed (3dmerge) to a 2.0mm using a Gaussian FWHM kernel. Each run was also despiked to further reduce the influence of motion on the data (3dDespike). Finally, functional data were normalized to percent change from baseline by subtracting mean signal from each voxel within a volume and dividing the result by 100 (3dTstat and 3dcalc). Functional scans were aligned to each subject's skull-stripped MP-RAGE (align_epi_anat.py). We defined ROIs in the medial temporal lobes (MTL) based on our prior work (Reagh et al., 2014; Yushkevich et al., 2015), and cortical regions were defined based on the Freesurfer image analysis suite (Dale, Fischl, & Sereno, 1999; Fischl, Sereno, & Dale, 1999) (available online at http://surfer.nmr.mgh.harvard.edu/) as well as anatomical atlases of human brain tissue (Mai, Voss, & Paxinos, 2008). Our anterior cingulate cortex (ACC) and ventromedial prefrontal cortex (vmPFC) ROI (ACC/vmPFC) was created based on anatomical atlases (Mai, Voss, & Paxinos, 2008) and Freesurfer's cingulate label. We combined ACC with a portion of vmPFC corresponding to Brodmann area 25 (the latter is analogous to agranular medial prefrontal cortex in rats, see Uylings & van Eden, 1990 and Öngür & Price, 2000) given the proximity and contiguity of these cortical regions. We segmented our thalamic nucleus reuniens (NR) ROI using an anatomical atlas based on human histological atlases (Mai, Voss, & Paxinos, 2008). Given the relatively small size of NR, we chose to center our ROI on the approximate location of NR and liberally include additional thalamic voxels near the third ventricle (See Fig. 3A). This almost surely includes some thalamic voxels outside NR, but critically, NR was undoubtedly included in the ROI. We used Advanced Normalization Tools (ANTS) (Avants et al., 2008) to warp each individual participant's MP-RAGE structural scan into our custom in-house high-resolution template space using nonlinear, diffeomorphic transformation. Parameters from these warps were used to also warp functional scans into template space for group analyses. Masks were resampled to match the resolution of the fMRI data (1.8×1.8. ×2.0mm) and were further masked to exclude partially sampled voxels within and across runs (3dcalc).

Resting state functional connectivity analyses proceeded similarly. Briefly, for the specific steps taken in AFNI, data were despiked (3dDespiked), slice timing corrected (3dtshift), aligned (align_epi_anat.py), motion corrected (3dvolreg), blurred to 2mm isotropic (3dmerge) with a Gaussian FWHM kernel, and automasked to exclude voxels outside the brain (3dautomask). Critically, in accordance with Power et al. (2012), we additionally regressed signal in white matter and ventricles to account for global signal related to motion and scanner artifact using ANATICOR (Jo et al., 2010). Once we obtained models of ongoing BOLD activity per subject (3dDeconvolve), we extracted the average time course across NR (3dmaskave) and calculated the cross-correlation of the resting state dataset with the reference time series in NR (3dfim+). The resultant correlation map was z-scored for each subject (3dcalc), and the z-scored functional connectivity maps were tested against zero at the group level (3dttest++). A control analysis using these same steps was conducted using a whole-thalamus mask rather than our specific NR ROI.

fMRI data analysis: general linear model regression

Only test data are included in the analyses here. For target trials, we constructed a general linear model (GLM) with regressors for number of exposures (1Enc vs. 3Enc) and accuracy (hit vs. miss) as fixed factors (given the finite range of levels of the conditions). For lure trials, a similar GLM was created with regressors for number of exposures (1Enc vs. 3Enc) and accuracy (correct rejection vs. false alarm). For both approaches, subject was entered as a random factor. These analyses were conducted in AFNI using 3dDeconvolve. Deconvolution of the hemodynamic response was done using tent functions covering stimulus onset to 15 seconds after onset with 6 estimator functions distributed across this time window. Motion parameters were entered into the model as explicit regressors to reduce the influence of motion on task-related parameter estimates. For all functional runs, TRs with motion exceeding 0.5mm frame displacement (but below our exclusion threshold of 3mm) were censored from analyses, as well as the immediately preceding and following TRs. These data scrubbing procedures were employed to rigorously exclude the potential effects of head motion on activation profiles (Power et al., 2012).

Final parameter estimates entered into second-level analyses consisted of the average of the first three estimator functions (targeted to capture the peak of the BOLD response). These parameter estimates were extracted from ROIs (note: beta weights converted to percent signal change via 3dcalc) for quantitative comparisons (3dmaskave). For a schematic of our ROI masks, see Fig. S1. Differences across conditions were assessed via 2 (1Enc vs. 3Enc) × 3 (Hits vs. CRs vs. FAs) repeated measures ANCOVAs, where decision criterion differences were modeled as a covariate. We did not model target misses because too few of these trials occurred, particularly in the 3Enc condition. Given that our ROIs were determined on purely anatomical bases, we note that we did not adjust our significance threshold across ROIs. That is, we did not adjust our critical p-value for each ANOVA performed within each individual ROI as these tests examined task effects within independently selected regions (see Poldrack & Mumford, 2009; Vul et al., 2009). We did, however, correct for multiple comparisons within ROIs such that pairwise comparisons were adjusted via Holm-Šidák post-hoc tests. In other words, significance thresholds for omnibus F statistics were not corrected across regions, but the critical alpha of 0.05 was adjusted to account for post-hoc comparisons within regions.

fMRI data analyses: interregional correlations and interactions

We performed context-dependent correlation analysis, also termed generalized psychophysiological interaction analysis (PPI) analyses (McLaren et al., 2012) over the test data for both target recognition and lure discrimination. A detailed walkthrough of these analysis steps in AFNI can be found here: (https://afni.nimh.nih.gov/sscc/gangc/CD-CorrAna.html). Briefly, a positive correlation indicates a positive relationship between significant voxels and a seed region *in a given condition*, whereas a negative correlation indicates a negative relationship. For target recognition, we examined trials in which correctly identified target items were initially studied once versus three times. We generated a seed time series in left anterior CA1 (3dmaskave) and detrended the time series (3dDetrend) (this seed time series features the same data scrubbing steps discussed previously). After transposing the detrended time series as a column vector (1dtranspose),

we generated a canonical HRF (waver) and used this to extract the expected contributions of BOLD signaling to the time series and generate an up-sampled “neural time series” (3dTfitter). We next multiplied the resulting “neural time series” with stimulus timing files (timing_tool.py and 1deval), which were finally convolved with the canonical HRF to create the interaction regressor (waver). This regressor was entered into a GLM (3dDeconvolve), where the ensuing beta weights reflect the degree of context-dependent correlations with the seeded region. To limit the impact of voxels on the edge of the functional acquisitions whose susceptibility to motion and partial volumes can induce spurious correlations, we removed outermost edge voxels from the correlation maps prior to the regression analysis (3dZeropad). For lures, the same steps were taken except we seeded left pDG/CA3 for the physiological variable, and we used 1Enc and 3Enc correct rejections and 1Enc and 3Enc false alarms as contextual/psychological variables.

For the purposes of visualizing correlational structures across the brain, PPI analyses (and resting state analyses) proceeded as voxel-based rather than ROI-based analyses. We note that in these cases we employed the appropriate statistical corrections. Individual subject maps were brought together and analyzed at the group level using t-tests (3dttest++). Voxels in the group analysis were considered significant at $p < 0.05$ corrected via familywise error rate (3dClustSim, modeled with 2 mm smoothed voxels yielding a $p = 0.05$ corrected with a cluster threshold of 51 contiguous voxels; note that this analysis was performed after the recent bug fix for 3dClustSim). Illustrative voxels in statistical maps displayed in Figures 3a-c and 6a-c were thresholded as such. We note that, for these analyses, raw beta weights were used rather than the scaled values reflecting percent change from baseline. While normalizing to percent signal change does not qualitatively alter the underlying data, we used raw beta weights here simply to capture the maximal extent of signal variability within subjects.

For mediation analyses, we modeled with the assumption of directionality from ACC/vmPFC to NR to aCA1, and from ACC/vmPFC to aCA1 (this assumption of directionality is a consequence of mediation analysis, and does not necessarily reflect underlying biological principles). We used the ‘mediation’ package in R to conduct these analyses, which given inputs of regression coefficients (raw beta weights, as was used in the PPI analysis) resulting from univariate GLMs across subjects, modeled the aforementioned pathways. The critical tests of mediation are (a) that the dependent variable (aCA1) is correlates with the independent variable (ACC/vmPFC), (b) that the independent variable correlates with the mediator (NR), (c) that the mediator correlates with the dependent variable, and finally (d) that the significance of the correlation between the dependent variable and the independent variable is contingent on the mediator. ‘Complete’ mediation is a result in which this is the case, whereas ‘incomplete’ mediation is a result in which the independent and dependent variables significantly correlate even when the influence of the mediator is accounted for.

An additional test used to assess this relationship was the Sobel test (Sobel, 1982). Generally, this test uses a specialized t-test to assess the extent to which a mediator variable accounts for variance in the correlational structure between an independent variable and a dependent variable. The test takes the raw regression coefficients between the independent variable and the mediator (ACC-vmPFC and NR) and between the mediator and the

dependent variable (NR and aCA1), as well as the standard errors of the regression coefficients. Formally, the test statistic is defined as:

$$\frac{a * b}{\sqrt{(b^2 * s_a) + (a^2 * s_b)}}$$

where 'a' refers to the independent variable to mediator pathway, 'b' refers to the mediator to dependent variable pathway, and 's_a' and 's_b' refer to the respective standard errors of these pathways. As opposed to the indirect method of assessing the significance of a fit coefficient before and after accounting for a mediator we previously described, the Sobel test explicitly probes the extent of mediation.

Statistical analysis

All statistical analyses on voxel-averaged data and data visualizations were conducted in R (version 3.2.4) and GraphPad Prism (Version 6.07). We conducted paired t-tests and factorial ANCOVAs in R using the t.test and aov functions. These tests are in general appropriate for conducting pairwise and factorial comparisons, respectively, and their assumptions of normality and homogeneous distribution of variance are not significantly violated in our data (Levene's test for equality of variances, all $p > 0.05$). Mediation analyses were performed in R using standard routines in the mediation toolbox. Preprocessing and first-level analyses of neuroimaging data were conducted in AFNI (Version 16.0) using the functions described throughout the Methods section. All fMRI statistical maps were corrected for multiple comparisons to an adjusted false positive rate of 5% overall using the familywise error (FWE) correction. All behavioral analyses were corrected for multiple comparisons using the Holm stepwise correction, or the Holm-Šidák method (conducted in Prism) where appropriate.

All analyses we report used established algorithms and programs in R, GraphPad Prism, and AFNI. Their usage as applied can be found throughout the Methods section. Custom python scripts (using NumPy and Pandas modules) were used to extract and designate the timing of stimulus delivery, and to format output files for subsequent analyses.

Results

Repetition increases both target recognition and lure false alarms

A schematic of the task is shown in Figure 1a, and a more detailed description can be found in the Methods. Briefly, subjects incidentally encoded pictures of common objects once (1Enc) or three times (3Enc) with "indoor/outdoor" judgments. Afterwards, a surprise test phase consisting of studied targets, similar (but not identical) lures, and entirely novel foils was completed with "same/different" judgments. Importantly, targets and lures were divided evenly into 1Enc and 3Enc trials based on whether the original item was presented only once or three times during the study phase.

We analyzed behavioral data in terms of proportion of hits ("same"|target) and correct rejections ("different"|lure). We analyzed simple proportions of correct responses, and

behavioral results are shown as a replication of our previously reported effect (Reagh & Yassa, 2014). We used a two-tailed paired t-test to compare target hits between 1Enc and 3Enc conditions. Recognition for 3Enc trials was greater than for 1Enc trials ($t(16) = 5.075$, $p < 0.001$) (Fig. 1b). Lures were distributed among 5 lure 'bins' corresponding to mnemonic similarity (with respect to the originally studied item) (Lacy et al., 2011; Yassa et al., 2011). A 2×5 repeated measures ANOVA (repetitions × lure bins) revealed significant effects of repetition ($F(1,16) = 17.93$, $p < 0.001$) and lure bin ($F(4,64) = 97.05$, $p < 0.001$), as well as an interaction ($F(4,64) = 5.795$, $p < 0.001$). Parsing the interaction, post hoc Holm-Šidák tests revealed that discrimination performance was better for 1Enc lures than 3Enc lures in bins 2, 3, and 4 (all $p < 0.05$ corrected). We also calculated area under the curve (AUC) summary value for each participant across lure bin performance (see Methods). Overall lure rejection rates were lower for 3Enc trials than for 1Enc trials ($t(16) = 2.524$, $p = 0.023$) (Fig. 1b). Thus, while repeated study enhanced target recognition, it also increased false alarms to similar lures. We observed a difference in decision criterion applied to target hits ($t(16) = 11.11$, $p < 0.001$) and lure rejections ($t(16) = 10.51$, $p < 0.001$) as a function of repetition. While this complicates interpretations about the nature of memory representations in the task per se, we explicitly covaried this difference in our fMRI analyses such that any significant effects exist beyond the influence of a possible criterion shift (see Methods)

Hippocampal and neocortical regions sensitive to repetition and memory decision

We examined the neural correlates of the above behavioral effects with high-resolution fMRI. Briefly, we defined ROIs in the MTL and hippocampal subfields based on our prior work (Reagh et al., 2014; Yushkevich et al., 2015). Cortical regions were selected from those described by Ritchey, Libby, and Ranganath (2015), and were defined based on the Freesurfer image analysis suite (Dale, Fischl, & Sereno, 1999a; Fischl, Sereno, & Dale, 1999b) and anatomical atlases of human brain tissue (Mai, Voss, & Paxinos, 2008). As previously noted, we additionally included a novel NR ROI, given its purported role in facilitating communication between the hippocampus and neocortex. ROIs are displayed in Figure S1.

Data were first analyzed via ROI-specific 2 (1Enc, 3Enc) × 3 (hits, lure correct rejections, and lure false alarms) repeated measures ANCOVAs with decision criterion as a covariate (see Methods). All significant effects and comparisons across conditions are summarized in Table 1, and are displayed in Figures 2 (anterior regions) and 3 (posterior regions).

Anterior hippocampal and cortical ROIs showing significant effects include left PRC, left NR, bilateral ACC/vmPFC, and left aCA1 (Fig. 2). In left PRC, we observed significant effects of repetition ($F(1,16) = 16.69$, $p < 0.001$) and condition ($F(2,32) = 4.310$, $p = 0.022$). In left NR, we observed only a significant effect of repetition ($F(1,16) = 14.78$, $p = 0.001$). In left ACC/vmPFC, we observed a significant effect of repetition ($F(1,16) = 25.16$, $p < 0.001$), condition ($F(2,32) = 7.840$, $p = 0.002$), as well as an interaction ($F(2,32) = 11.71$, $p < 0.001$). Right ACC/vmPFC featured a significant effect of repetition ($F(1,16) = 5.813$, $p = 0.028$) and an interaction ($F(2,32) = 3.703$, $p = 0.036$). Finally, left aCA1 showed significant effects of repetition ($F(1,16) = 10.67$, $p = 0.005$) and condition ($F(2,32) = 3.345$, $p = 0.048$).

Posterior hippocampal and cortical ROIs showing significant effects include bilateral pDG/CA3, bilateral PHC, and left RSC (Fig. 3). In left pDG/CA3, we observed a significant effect of condition ($F(2,32) = 3.517$, $p = 0.042$) and an interaction ($F(2,32) = 6.410$, $p = 0.005$). Right pDG/CA3 showed only an interaction ($F(2,32) = 3.905$, $p = 0.031$). In left PHC, we observed significant effects of repetition ($F(1,16) = 5.075$, $p = 0.039$) and condition ($F(2,32) = 3.873$, $p = 0.031$), as well as an interaction ($F(2,32) = 7.313$, $p = 0.002$). In right PHC, we found only a significant interaction ($F(2,32) = 5.753$, $p = 0.007$). Finally, in left RSC, we found a significant effect of condition ($F(2,32) = 4.752$, $p = 0.016$) and an interaction ($F(2,32) = 5.495$, $p = 0.009$).

Repetition shifts engagement of anterior regions during accurate and inaccurate recognition (target hits and false alarms)

Having established that subfields of the hippocampus – left aCA1 and bilateral pDG/CA3 – as well as several anterior and posterior cortical regions were sensitive to both repeated study and retrieval condition, we next examined specific response profiles in post hoc comparisons. Holm-Šidák tests revealed significant differences between 1Enc and 3Enc target hits in left PRC, left NR, bilateral ACC/vmPFC, and left aCA1 ($p < 0.05$ corrected). We observed increased activation during 3Enc compared to 1Enc target hits in anterior cortical regions (Fig. 2a-d), and decreased activation in aCA1 (Fig. 2e) in the same comparison. Additionally we observed increased activation during 3Enc compared to 1Enc false alarms in left PRC and ACC/vmPFC ($p < 0.05$ corrected) (Fig. 2a&c). Importantly, repetition-related increases in activity in anterior regions were similar across target hits and false alarms, suggesting that they make share common neural correlates. The left PRC and ACC/vmPFC were additionally more active during 3Enc false alarms compared to 3Enc correct rejections ($p < 0.05$ corrected), suggesting that they may contribute to dissociating well-learned stimuli as well. No anterior ROIs significantly differentiated 1Enc target hits from lure rejections, but left PRC, left ACC/vmPFC, and left aCA1 did so for 3Enc trials (all $p < 0.05$ corrected). Overall, repetition was associated with general increases in activation in anterior cortical regions including PRC and ACC/vmPFC and decreased activation in the aCA1 during recognition.

Repetition shifts engagement of posterior regions during lure discrimination

Post hoc Holm-Šidák tests revealed significant differences between 1Enc and 3Enc correct rejections as well as differences between correct rejections and false alarms in bilateral pDG/CA3, bilateral PHC, and left RSC (all $p < 0.05$ corrected). Bilateral pDG/CA3 (Fig. 3a&b) differentiated between correct rejections and false alarms for 1Enc ($p < 0.05$ corrected), but not for 3Enc trials. Conversely, bilateral PHC (Fig. 3c&d) and left RSC (Fig. 3e) differentiated between correct rejections and false alarms for 3Enc trials (all $p < 0.05$ corrected) but not for 1Enc trials. Finally, contrasting discrimination versus recognition, bilateral pDG/CA3 showed significantly greater engagement during 1Enc correct rejections than 1Enc target hits, whereas bilateral PHC and left RSC showed greater engagement during 3Enc correct rejections than 3Enc target hits (all $p < 0.05$ corrected). Overall, repetition was associated with decreased activation in pDG/CA3 and increased activation in posterior cortical areas including PHC and RSC during lure discrimination.

Response profiles in in pDG/CA3 and PHC are modulated by lure similarity

We next examined the effects of lure similarity (high vs. low, with respect to the original image) in correct rejections and false alarms across the posterior ROIs discussed above. These analyses used 2 (repetition) × 4 (condition: hi-sim correct rejections and false alarms, and lo-sim correct rejections and false alarms) repeated measures ANOVAs followed by post hoc Holm-Šidák tests (Fig. 3). In left pDG/CA3, we observed significant effects of condition ($F(3,48) = 3.020$, $p = 0.039$) and repetition ($F(1,16) = 5.113$, $p = 0.038$), as well as an interaction ($F(3,48 = 2.984$, $p = 0.041$) (Fig. 3a). Post-hoc comparisons revealed significantly greater engagement during 1Enc trials than 3Enc trials for hi-sim and lo-sim correct rejections ($p < 0.05$ corrected). Moreover, we found greater engagement during hi-sim and lo-sim correct rejections than false alarms in the corresponding similarity bins ($p < 0.05$ corrected). In right pDG/CA3, we found significant effects of condition ($F(3,48 = 6.194$, $p = 0.001$) and repetition ($F(1,16) = 5.721$, $p = 0.029$) (Fig. 3b). In right pDG/CA3, we found only a significant difference between correct rejections and false alarms for hi-sim lures ($p < 0.05$ corrected), though the response profile overall was highly similar to left pDG/CA3. We found a significant effect of condition in both the left PHC ($F(3,48) = 3.283$, $p = 0.029$) and right PHC ($F(3,48) = 4.634$, $p = 0.006$) (Fig. 3c&d). Moreover, in both regions, we found greater engagement during lo-sim correct rejections compared to lo-sim false alarms, as well as hi-sim correct rejections in the 3Enc condition (all $p < 0.05$ corrected). In contrast with the ANOVA collapsed across similarity, we did not observe any significant effects in left RSC. In sum, these analyses revealed distinct interference-based response profiles in hippocampal pDG/CA3 and PHC, which were modulated by repetition. Whereas pDG/CA3 dissociated correct rejections from false alarms across similarity levels for singly studied items, this effect was not present for triply studied items. Conversely, in PHC, only 3Enc items featured a correct rejection versus false alarm dissociation, and only for low similarity items.

Correlations between vmPFC/ACC, NR, and aCA1 during recognition of repeated stimuli

In order to examine functional connectivity among the above hippocampal-neocortical subregions, we performed a context-dependent correlational analysis, also called psychophysiological interaction analysis (McLaren et al., 2012) (PPI; see Methods for details). Using the left ACC/vmPFC as a seed region and repetition of target hits (1Enc vs. 3Enc) as the contextual variable, we found a significant positive context-dependent correlation between left ACC/vmPFC and left NR, as well as a negative correlation between left ACC/vmPFC and left aCA1 during recognition of 3Enc targets (all $p < 0.05$ corrected) (Fig. 3a-c). This correlational pattern was not observed during 1Enc target hits, suggesting that repetition influences coordination of activity. This pattern of enhanced functional connectivity aligns with the known anatomical connectivity among these regions (Varela et al., 2014; Vertes et al., 2007; Griffin, 2015). Corroborating this finding, we performed a similar context-dependent correlation analysis seeding NR, and observed significant task-related correlations with both aCA1 and ACC/vmPFC (Fig. S2). A control analysis using a whole thalamus ROI (based on Freesurfer's subcortical aseg protocol) excluding voxels in the NR ROI did not reveal such correlations. This suggests that this pattern of connectivity is specific to the NR subregion and not the remainder of the thalamus.

Prefrontal-hippocampal correlations during recognition of repeated stimuli are mediated by NR

Given that we observed significant task-related functional connectivity among left ACC/vmPFC, NR, and aCA1, we next asked whether – as might be expected from current theories (Griffin, 2015) – activity in NR influences relationships between medial prefrontal regions and the hippocampus. To test this, we performed a mediation analysis assuming directionality from ACC/vmPFC to aCA1 in the direct pathway and ACC/vmPFC to NR to aCA1 in the mediated pathway. Importantly, the directionality was necessarily assumed only for the mediation model and was not intended to be a reflection of true structural anatomical connectivity. We chose to assess activity in the left hemispheric ROIs given the greater consistency of effects than those observed in ROIs in the right hemisphere in our data. Separate analyses were run for 1Enc and 3Enc target hits.

For the 1Enc condition, no regression coefficients modeling influences across ROIs were significant, though the direct ACC/vmPFC beta was marginal ($\beta = -0.608$, $t(16) = 1.772$, $p = 0.097$) (Fig. 4d). In contrast, for the 3Enc condition, the modeled connection between ACC/vmPFC and NR was significantly predictive ($\beta = 1.311$, $t(16) = 3.077$, $p = 0.008$), as were those between NR and aCA1 ($\beta = -1.077$, $t(16) = 2.577$, $p = 0.021$) and directly between ACC/vmPFC and aCA1 when modeled without NR as a mediator ($\beta = -0.843$, $t(16) = 2.416$, $p = 0.028$). Critically, however, when accounting for the pathway mediated by NR, the ACC/vmPFC to aCA1 connection was no longer significant ($\beta = -0.693$, $t(16) = 1.862$), $p = 0.081$) (Fig. 4e). Though the latter effect is marginal, warranting cautious interpretation, this demonstrates that NR significantly mediated the correlational structure of ACC/vmPFC to aCA1.

To further test the extent to which NR might be mediating interactions between ACC/vmPFC and aCA1, we performed a Sobel test (Sobel, 1982) on the 1Enc and 3Enc mediation models. Briefly this method uses a specialized t-test to assess the significance of the influence of the mediator variable (NR) on the dependent variable (aCA1) beyond direct influences from the independent variable (ACC/vmPFC). This test was not significant during 1Enc target hits ($t = -0.627$, $p = 0.531$), but was significant during 3Enc target hits ($t = -2.411$, $p = 0.016$) (Fig. 4d&e). This further demonstrates a role of NR in mediating context-dependent correlations among ACC/vmPFC and aCA1.

Resting state functional connectivity of NR reveals coupling with ACC/vmPFC and the hippocampus along its longitudinal axis

To further explore the correlational structure of these regions, we tested functional connectivity in separate resting state scans collected during the same scan sessions for each subject using NR bilaterally as a seed region. Briefly, data were preprocessed and were ‘scrubbed’ for motion and scanner related artifacts (Power et al., 2012; see Methods for further details). Normalized (z-scored) group functional connectivity results are displayed in Fig. S4. At a corrected threshold (FWE alpha = 0.05, cluster threshold of 51 contiguous voxels), we observed significant correlations between NR and bilateral ACC/vmPFC, as well as the hippocampus bilaterally along its longitudinal axis (Fig. 5a). This is in contrast to the anterior hippocampus-specific effects of repetition we report above, although consistent with

the fact that NR is anatomically connected along the entire hippocampal axis (Varela et al., 2014). As a control analysis, we reassessed functional connectivity using a whole-thalamus mask excluding our NR ROI. This revealed a very different and more widespread correlational pattern which – even at a liberal threshold of $p = 0.05$ uncorrected – did not include the hippocampus or the ventromedial portion of PFC (Fig. 5b).

Enhanced connectivity between pDG/CA3 and posterior areas during lure discrimination, and anterior areas during false recognition

As we did with recognition, we performed a context-dependent correlational analysis, this time using pDG/CA3 as a seed region and 3Enc vs. 1Enc correct rejections and false alarms as the contextual variables. We focused on left pDG/CA3 (Fig. S3a) given the more statistically reliable findings in the prior analysis in this ROI compared to the right ROI. For 3Enc false alarms, we found significant negative context-dependent correlations between left pDG/CA3 and left anterior hippocampus (including CA1 and subiculum) and PRC (Supplemental Fig. 3b) ($p < 0.05$ corrected). Conversely, we found significant negative correlations between left pDG/CA3 and bilateral PHC and RSC during 3Enc lure rejections ($p < 0.05$ corrected) (Fig. S3c&d). Thus, with repetition, posterior hippocampal and cortical regions were negatively correlated during lure discrimination but not during false recognition, whereas pDG/CA3 correlated negatively with anterior regions. Similar to the target recognition results, we did not observe significant interregional correlations during 1Enc lure false alarms or rejections, further suggesting that repetition drove the correlational structure observed here. We note that, despite the observed correlations in BOLD signal, structural connectivity between the MTL and the RSC occurs largely through the entorhinal cortex. However, anatomical connections between the hippocampus, PHC, and RCS have been reported (Sugar et al., 2011). We did not observe significant modulations or correlations in entorhinal cortex in this dataset, likely due to MRI signal dropout in this region across a number of the subjects we analyzed.

Discussion

Here, we describe a high-resolution fMRI study designed to assess hippocampal-neocortical network engagement and connectivity during retrieval of repeatedly studied information. Replicating our previously reported behavioral effect (Reagh & Yassa, 2014), we found that repetition led to enhanced recognition memory and poorer lure discrimination performance. Repetition-related enhancements in target recognition were associated with reduced aCA1 engagement and increased anterior cortical engagement, including ACC/vmPFC. Repetition-related decreases in lure discrimination were associated with reduced pDG/CA3 engagement and enhanced posterior cortical engagement. Moreover, we found task-related functional interactions among these respective networks, and we report evidence for a functional role of thalamic NR in mediating hippocampal-prefrontal interactions in humans. Overall, these data provide novel insight into the way the brain responds to repeated encoding, and suggests hippocampal-neocortical shifts in distinct networks for recognition and discrimination judgments.

Repetition reveals recognition versus discrimination effects in hippocampal-neocortical networks

A major motivation of this experiment was to determine the neural correlates of the discrepancy between enhanced recognition and diminished discrimination with repetition. Though repetition has been studied in the context of discrimination memory, some prior investigations have not observed such a discrepancy (Hintzman, Caulton, & Levitin; 1998). Unlike these tasks, which largely use words as stimuli, the objects used in our paradigm may have featured a perceptual richness that allowed for greater nuance to emerge in terms of repetition-related effects at retrieval.

What mechanisms underlie this phenomenon? As repetition increased both true and false recognition, and given that these judgments coincided with engagement of anterior cortices, our data are consistent with a shift towards a familiarity-based retrieval process (Yonelinas, 2002). Indeed, it has been previously reported that repeated study shifts response contingencies from “remember” (a behavioral proxy for detailed ‘recollection’) to “know” (a behavioral proxy for familiarity) (Reder et al., 2000). PRC has been particularly related to mnemonic decisions guided by familiarity and memory strength in the absence of distinctive information about items (Jenkins & Ranganath, 2016). Unlike anterior regions we examined, posterior cortices showed repetition-related enhancements specific to discrimination memory. Accumulating evidence favors a view that anterior and posterior brain systems serve distinct roles in memory (Ritchey, Libby, & Ranganath, 2015). In particular, such theories have largely proposed that anterior brain regions serve generalized processing, whereas posterior regions operate over finer-grained representations. Discriminating a present stimulus from a related stimulus in memory likely relies on a more detailed representation than lumping that stimulus into an existing category (Van Kesteren et al., 2012). Thus, our results of anterior recognition signals and posterior discrimination signals in cortical areas are highly consistent with extant frameworks.

The hippocampus is thought to participate in the encoding of ‘episodes’ consisting of interlinked features. Over time, information from hippocampus-dependent episodes is thought to become incorporated into cortical networks (Winocur & Moscovitch, 2011; Nadel et al., 2012). This likely occurs by extracting categories and regularities, or ‘schemas,’ across episodes (van Kesteren et al., 2012). Recent studies in rodent models (Tse et al., 2007; Tse et al., 2011) and humans (van Kesteren et al., 2009; van Kesteren et al., 2013; Sommer, 2016) suggest that novel information can more be more readily encoded using existing neocortical traces if the information is schema-consistent, which furthermore accords with the CLS model of the roles of the hippocampus and neocortex (McClelland, 2013).

Given that our stimuli are common objects that are consistent with many existing schemas (e.g., ‘telephone’), it is possible that repeated study facilitated an accelerated acquisition by neocortical areas supporting memory for the objects in the task (though the extent to which this process may be obligatory or automatic is unclear). Moreover, as discussed above, the regions of the hippocampus and neocortex involved in this representational shift may depend on the type or scale of information being remembered. The hippocampus is also thought to exhibit a gradation of scale/precision of representation along its longitudinal axis (Poppenk

et al., 2013; Strange et al., 2014), and our dissociation of recognition engaging the anterior hippocampus and discrimination engaging the posterior hippocampus (which may reflect an increased demand on pattern separation; see Schlichting, Mumford, & Preston, 2015) is consistent with this perspective. In sum, repeated study may shift largely hippocampus-mediated representations to neocortical regions, and this may differ regionally as a function of precision or detail. In terms of cognitive or behavioral consequences, this shift towards cortical engagement manifests as an increased reliance on a familiarity-based process supported by anterior cortices, whereas posterior cortices supporting 'recollection' increase their involvement in facilitating discrimination memory (Jacoby, Wahlheim, & Yonelinas, 2013).

The role of human thalamic NR in mediating anterior CA1-ACC/vmPFC connectivity

A key finding of the current study is that thalamic NR mediated connectivity between CA1 and ACC/vmPFC during recognition of repeated stimuli. In our data, we observed a positive correlation between ACC/vmPFC and NR, and a negative correlation between these regions and aCA1. This may indicate coordination between ACC/vmPFC and NR under conditions of repeated study that relates to the reduced engagement we observed in aCA1. As NR is thought to be a critical means of information transfer between the prefrontal cortex and hippocampus (Varela et al., 2014; Vertes et al., 2007; Griffin, 2015), our results are consistent with known anatomical and functional roles. Importantly, this circuit has been implicated in memory transformation or "consolidation" in the context of animal studies (Goshen et al., 2011) and computational models (Ketz, Jenson, & O'Reilly, 2015). It has also been implicated in generalization of fear responses (Xu & Sudhof, 2013) as well as spatial navigation (Ito et al., 2015). It is likely that this circuit is involved in several aspects of memory processing and is central to how hippocampal-neocortical traces are established and altered over time. To our knowledge, these results are among the first evidence in humans that the thalamic NR is an important region in this memory network.

It bears mentioning that our PPI results showed only anterior hippocampal correlations with NR, whereas resting state functional connectivity showed correlations with the hippocampus along its entire longitudinal axis. There are in fact anatomical connections along the entire hippocampal extent with NR in rodents, though projections are densest in the anterior (ventral) hippocampus (Vertes et al., 2007). The emphasis on the anterior hippocampus in the PPI results is likely due to the fact that 3Enc target hits were specifically being modeled. As can be seen from our univariate fMRI results, target hits involved the anterior but not the posterior portion of the hippocampus (Fig. 2).

Limitations of the current study

A limitation of our study imposed by the nature of the BOLD response is that increases and decreases in activity cannot be taken to exclusively reflect the degree to which a brain region is involved in a specific process. For example, the increase in cortical involvement – seemingly at the expense of hippocampal involvement – can arise from two main possibilities: 1) sharpening of hippocampal representations used to index neocortical areas (from the perspective of BOLD fMRI, an *apparent* decrease in hippocampal engagement), or 2) an *actual* and not merely apparent decrease in hippocampal engagement. In the absence of

a more sensitive measure of the activity of discrete neuronal ensembles from techniques such as high-density array neurophysiology, we cannot adjudicate between these possibilities.

It is important to note that we did find evidence for a difference in decision criterion applied to target hits and lure rejections as a function of repetition. The difference we observed implies that, although encoding was incidental, repetition was associated with a systematic shift toward endorsing multiply studied items as old for both targets and lures at test. Though this limits strong interpretations of how the behavioral results bear on memory representations, the net result of an increased tendency to endorse any repeated information as being old is an interesting mnemonic phenomenon. Furthermore, we note that by covarying the criterion difference across conditions in our neuroimaging analyses, we have accounted for this effect in assessing task-associated effects across brain regions. Thus, response profiles across brain regions are assessed and reported in a way that accounts for the influence of any systematic differences in behavior.

Another limitation is that, although our high-resolution functional scans captured the majority of the brain (Fig. S4), several memory-related regions were outside the field of view, including some of the dorsolateral prefrontal cortices and the superior parietal lobules. These regions could potentially show response profiles comparable to the regions we examined here, but our field of view was too restricted to examine them. Finally, as previously noted, the object stimuli used in our task likely have existing ‘schemas’ already associated with them. Though we cannot address this in the present data, an interesting future experiment would be to examine, both behaviorally and neurally, how repetition may affect the encoding of abstract objects (e.g. kaleidoscopic stimuli) for which there is not an existing ‘schema.’

Summary

These results provide novel evidence for distinct brain circuits and networks underlying enhanced recognition and diminished discrimination memory with repeated study. We demonstrate that repeated study can, even in a brief period of time (under an hour), shift the relative balance of hippocampal-neocortical engagement, depending on the specificity of the associated mnemonic judgment, and that the shift is distributed across the hippocampal long axis. Finally, we demonstrate novel evidence for a functional memory-related role of thalamic NR in the human brain.

Supplementary Material

Refer to Web version on PubMed Central for supplementary material.

Acknowledgments

This research was supported by US NIA P50 AG05146, NIA R21 AG049220, and NIMH R01 MH102392 (to M.A.Y.). Support for Z.M.R. provided by US NSF Graduate Research Fellowship DGE-1232825, and a fellowship from the ARCS and Roche Foundations. We thank Craig Stark, Derek Huffman, Jay McClelland, and Richard Morris for helpful discussions.

References

Abdi H. The Bonferonni and Šidák corrections for multiple comparisons. Encyclopedia of measurement and statistics. 2007; 3:103–107.

Aggleton JP. Multiple anatomical systems embedded within the primate medial temporal lobe: implications for hippocampal function. Neuroscience & Biobehavioral Reviews. 2011; 32:1579–1596.

Avants B, Duda JT, Kim J, Zhang HY, Pluta J, Gee JC, Whyte J. Multivariate analysis of structural and diffusion imaging in traumatic brain injury. Academic Radiology. 2008; 15(11):1360–1375. [PubMed: 18995188]

Binder JR, Desai RH. The neurobiology of semantic memory. Trends in Cognitive Science. 2011; 15:527–536.

Cox RW. AFNI: Software for analysis and visualization of functional magnetic resonance neuroimages. Computers and Biomedical Research. 1996; 29:162–173. [PubMed: 8812068]

Dale AM, Fischl Bruce, Sereno MI. Cortical surface-based analysis I: Segmentation and surface reconstruction. Neuroimage. 1999; 9(2):179–194. [PubMed: 9931268]

Dudai Y. The Neurobiology of Consolidations, Or, How Stable is the Engram? Annual Review of Psychology. 2004; 55:51–86.

Ebbinghaus H. A contribution to experimental psychology. New York: Teachers. 1913

Fischl BR, Sereno MI, Dale AM. Cortical surface-based analysis II: Inflation, flattening, and surface-based coordinate system. Neuroimage. 1999; 9(2):195–207. [PubMed: 9931269]

Gonzalez C, Kramar C, Garagoli F, Rossato JI, Weisstaub N, Cammarota M, Medina JH. Medial prefrontal cortex is a crucial node of a rapid learning system that retrieves recent and remote memories. Neurobiology of Learning and Memory. 2013; 103:19–25. [PubMed: 23608181]

Goshen I, Brodsky M, Prakash R, Wallace J, Gradinaru V, Ramakrishnan C, Deisseroth K. Dynamics of retrieval strategies for remote memories. Cell. 2011; 147(3):678–689. [PubMed: 22019004]

Griffin AL. Role of the thalamic nucleus reuniens in mediating interactions between the hippocampus and medial prefrontal cortex during spatial working memory. Frontiers in Systems Neuroscience. 2015; 9(29)

Hintzman DL. Repetition and memory. Psychology of Learning and Motivation. 1974; 10:47–91.

Hintzman DL, Caulton DA, Levitin DJ. Retrieval dynamics in recognition and list discrimination: Further evidence for separate processes of familiarity and recall. Memory & Cognition. 1998; 26(3):449–462. [PubMed: 9610117]

Holm S. A simple sequentially rejective multiple test procedure. Scandinavian journal of statistics. 1979:65–70.

Ito HT, Zhang SJ, Witter MP, Moser EI, Moser MB. A prefrontal-thalamo-hippocampal circuit for goal-directed spatial navigation. Nature. 2015; 522:50–55. [PubMed: 26017312]

Jacoby LL, Wahlheim CN, Yonelinas AP. Memory and Cognition. 2013; 41(5):638–649. [PubMed: 23529660]

Jenkins LJ, Ranganath C. Distinct neural mechanisms for remembering when an event occurred. Hippocampus. 2016; 26(5):554–559. [PubMed: 26845069]

Jo HJ, Saad ZS, Simmons WK, Milbury LA, Cox RW. Mapping sources of correlation in resting state fMRI, with artifact detection and removal. Neuroimage. 2010; 52(5):571–582. [PubMed: 20420926]

Ketz NA, Jenson O, O'Reilly RC. Thalamic pathways underlying prefrontal cortex-medial temporal lobe oscillatory interactions. Trends in Neurosciences. 2015; 38(1):1229–1248.

Lacy JW, Yassa MA, Stark SM, Muftuler LT, Stark CEL. Distinct pattern separation related transfer functions in human CA3/dentate and CA1 revealed using high-resolution fMRI and variable mnemonic similarity. Learning & Memory. 2011; 18:15–18. [PubMed: 21164173]

Leutgeb JK, Leutgeb S, Moser MB, Moser EI. Pattern separation in the dentate gyrus and CA3 of the hippocampus. Science. 2007; 315(5814):961–966. [PubMed: 17303747]

Libby LA, Ekstrom AD, Ragland JD, Ranganath C. Differential connectivity of perirhinal and parahippocampal cortices within hippocampal subregions revealed by high-resolution functional imaging. The Journal of Neuroscience. 2012; 32(19):6550–6560. [PubMed: 22573677]

Mai, JK., Voss, T., Paxinos, G. Atlas of the human brain. Amsterdam, Netherlands: Elsevier/Academic Press; 2008.

McClelland JL. Incorporating rapid neocortical learning of new schema-consistent information into complementary learning systems theory. Journal of Experimental Psychology General. 2013; 142:1190–1210. [PubMed: 23978185]

McClelland JL, McNaughton BL, O'Reilly RC. Why there are complementary learning systems in the hippocampus and neocortex: Insights from the successes and failures of connectionist models of learning and memory. Psychological Review. 1995; 102(3):419–457. [PubMed: 7624455]

McGaugh JL. Memory – a Century of Consolidation. Science. 2000; 287(5451):248–251. [PubMed: 10634773]

McLaren DG, Ries ML, Xu G, Johnson SC. A generalized form of context-dependent psychophysiological interactions (gPPI): A comparison to standard approaches. NeuroImage. 2012; 61(4):1277–1286. [PubMed: 22484411]

Meeter M, Murre JM. Consolidation of long-term memory: evidence and alternatives. Psychological Bulletin. 2004; 130:843–857. [PubMed: 15535740]

Nadel L, Hoscheidt S, Ryan LR. Spatial cognition and the hippocampus: The anterior-posterior axis. Journal of Cognitive Neuroscience. 2012; 25(1):22–28.

Nadel L, Hupbach A, Gomez R, Newman-Smith K. Memory formation, consolidation and transformation. Neuroscience & Biobehavioral Reviews. 2012; 36(7):1640–1645. [PubMed: 22465050]

Norman KA. How hippocampus and cortex contribute to recognition memory: Revisiting the complementary learning systems model. Hippocampus. 2010; 20(11):1217–1227. [PubMed: 20857486]

O'Reilly RC, Bhattacharyya R, Howard MD, Ketz N. Complementary Learning Systems. Cognitive Science. 2014; 38(6):1229–1248. [PubMed: 22141588]

Öngür D, Price JL. The organization of networks within the orbital and medial prefrontal cortex of rats, monkeys and humans. Cerebral Cortex. 2000; 10(3):206–219. [PubMed: 10731217]

Poldrack RA, Mumford JA. Independence in ROI analysis: where is the voodoo? Social Cognitive and Affective Neuroscience. 2009; 4(2):208–213. [PubMed: 19470529]

Poppenk J, Evensmoen HR, Moscovitch M, Nadel L. Long-axis specialization of the human hippocampus. Trends in Cognitive Sciences. 2013; 17(5):230–240. [PubMed: 23597720]

Power JD, Barnes KA, Snyder AZ, Schlagger BL, Petersen SE. Spurious but systematic correlations in functional connectivity MRI networks arise from subject motion. NeuroImage. 2012; 59(3):2142–2154. [PubMed: 22019881]

Quinn JJ, Ma QD, Tinsley MR, Koch C, Fanselow MS. Inverse temporal contributions of the dorsal hippocampus and medial prefrontal cortex to the expression of long-term fear memories. Learning & Memory. 2008; 15:368–372. [PubMed: 18441294]

Reagh ZM, Yassa MA. Repetition strengthens target recognition but impairs similar lure discrimination: Evidence for trace competition. Learning & Memory. 2014; 21:342–346. [PubMed: 24934334]

Reagh ZM, Watabe J, Ly M, Murray E, Yassa MA. Dissociated signals in human dentate gyrus and CA3 predict different facets of recognition memory. The Journal of Neuroscience. 2014; 34(40): 13301–13313. [PubMed: 25274810]

Reed JM, Squire LR. Retrograde amnesia for facts and events: Findings from four new cases. The Journal of Neuroscience. 1998; 18(10):3943–3954. [PubMed: 9570821]

Reder LM, Nhouyvanisvong A, Schunn CD, Ayers MS, Angstadt P, Hiraki K. A mechanistic account of the mirror effect for word frequency: a computational model of remember-know judgments in a continuous recognition paradigm. Journal of Experimental Psychology: Learning, Memory, and Cognition. 2000; 26(2):294–320.

Ritchey M, Libby LA, Ranganath C. Chapter 3 – Cortico-hippocampal systems involved in memory and cognition: the PMAT framework. Progress in Brain Research. 2015; 219:45–64. [PubMed: 26072233]

Ross RS, Eichenbaum H. Dynamics of hippocampal and cortical activation during consolidation of a nonspatial memory. The Journal of Neuroscience. 2006; 26:4852–4859. [PubMed: 16672659]

Schlichting ML, Mumford JA, Preston AR. Learning-related representational changes reveal dissociable integration and separation signals in the hippocampus and prefrontal cortex. Nature Communications. 2015; 6:8151.

Scoville WB, Milner B. Loss of Recent Memory After Bilateral Hippocampal Lesions. Journal of Neurology, Neurosurgery & Psychiatry. 1957; 20(1):11–21.

Sobel ME. Asymptotic confidence intervals for indirect effects in structural equation models. Sociological Methodology. 1982; 16:159–186.

Sommer T. The emergence of knowledge and how it supports the memory for novel related information. Cerebral Cortex. 2016

Strange BA, Witter MP, Lein ES, Moser EI. Functional organization fo the hippocampal longitudinal axis. Nature Reviews Neuroscience. 2014; 15:655–669. [PubMed: 25234264]

Sugar J, Witter MP, van Strien NM, Cappaert NLM. The retrosplenial cortex: Intrinsic connectivity and connections with the (para)hippocampal region in the rat. An interactive connectome. Frontiers in Neuroinformatics. 2011; 5(7)

Teyler TJ, DiScenna P. The hippocampal memory indexing theory. Behavioral Neuroscience. 1986; 100(2):147–154. [PubMed: 3008780]

Teyler TJ, Rudy JW. The hippocampal indexing theory and episodic memory: updating the index. Hippocampus. 2007; 17(12):1158–1169. [PubMed: 17696170]

Tse D, Langston RF, Kakeyama M, Bethus I, Spooner PA, Wood ER, Witter MP, Morris RG. Schemas and memory consolidation. Science. 2007; 316:76–82. [PubMed: 17412951]

Tse D, Takeuchi T, Kakeyama M, Kajii Y, Okuno H, Tohyama C, Bito H, Morris RG. Schema-dependent gene activation and memory encoding in neocortex. Science. 2011; 333:891–895. [PubMed: 21737703]

Uylings HB, van Eden CG. Qualitative and quantitative comparison of the prefrontal cortex in rat and in primates, including humans. Progress in Brain Research. 1990; 85:31–62. [PubMed: 2094901]

van Kesteren MT, Beul SF, Takashima A, Henson RN, Ruiter DJ, Fernandez G. Differential roles for medial prefrontal and medial temporal cortices in schema-dependent encoding: from congruent to incongruent. Neuropsychologia. 2013; 51:2352–2359. [PubMed: 23770537]

van Kesteren MT, Fernandez G, Norris DG, Hermans EJ. Persistent schema-dependent hippocampal-neocortical connectivity during memory encoding and postencoding rest in humans. Proceedings of the National Academy of Sciences. 2009; 107(16):7550–7555.

van Kesteren MT, Ruiter DJ, Fernandez G, Henson RN. How schema and novelty augment memory formation. Trends in Neurosciences. 2012; 35(4):211–219. [PubMed: 22398180]

Varela C, Kumar S, Yang JY, Wilson MA. Anatomical substrates for direct interactions between hippocampus, medial prefrontal cortex, and the thalamic nucleus reuniens. Brain Structure and Function. 2014; 219(3):911–929. [PubMed: 23571778]

Vertes RP, Hoover WB, Szigeti-Buck K, Leranth C. Nucleus reuniens of the midline thalamus: Link between the medial prefrontal cortex and the hippocampus. Brain Research Bulletin. 2007; 71(6): 601–609. [PubMed: 17292803]

Vul E, Harris C, Winkleman P, Pashler H. Puzzlingly high correlations in fMRI studies of emotion, personality, and social cognition. Perspectives on Psychological Science. 2009; 4(3):274–290. [PubMed: 26158964]

Wang SF, Ritchey M, Libby LA, Ranganath C. Functional connectivity based parcellation of the human medial temporal lobe. Neurobiology of Learning and Memory. (in press).

Wang SH, Teixeira CM, Wheeler AL, Frankland PW. The precision of remote context memories does not require the hippocampus. Nature Neuroscience. 2009; 12:253–255. [PubMed: 19182794]

Winocur G, Moscovitch M. Memory Transformation and Systems Consolidation. Journal of the International Neuropsychological Society. 2011; 17(5):766–780. [PubMed: 21729403]

Xu W, Sudhof TC. A neural circuit for memory specificity and generalization. Science. 2013; 339(6125):1290–1295. [PubMed: 23493706]

Xue G, Dong Q, Chen C, Lu Z, Mumford JA, Poldrack RA. Greater neural pattern similarity across repetitions is associated with better memory. Science. 2010; 330(6000):97–101. [PubMed: 20829453]

Yassa MA, Lacy JW, Stark SM, Albert MS, Gallagher M, Stark CEL. Pattern separation deficits associated with increased hippocampal CA3 and dentate gyrus activity in nondemented older adults. Hippocampus. 2011; 21(9):968–979. [PubMed: 20865732]

Yonelinas AP. The nature of recollection and familiarity: A review of 30 years of research. Journal of Memory and Language. 2002; 26:441–517.

Yushkevich, et al. Quantitative comparison of 21 protocols for labeling hippocampal subfields and parahippocampal subregions in in vivo MRI: towards a harmonized segmentation protocol. NeuroImage. 2015; 111:526–541. [PubMed: 25596463]

Zandbelt BB, Gladwin TE, Raemaekers M, van Buuren M, Neggers SF, Kahn RS, Ramsey NF, Vink M. Within-subject variation in BOLD-fMRI signal changes across repeated measurements: Quantification and implications for sample size. NeuroImage. 2008; 42(1):196–206. [PubMed: 18538585]

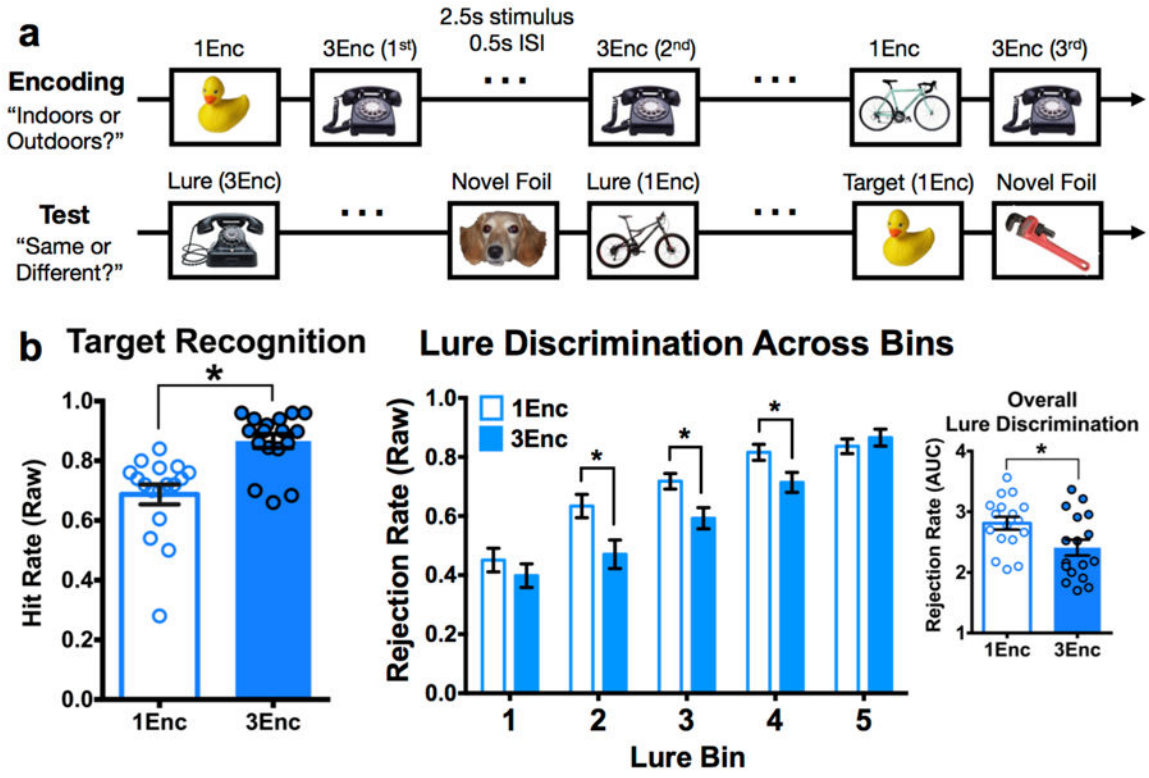

Figure 1. Repetition increases target hit rate and lure false alarm rate

(a) Schematic of the task. Participants first completed an encoding task with an incidental "Indoors or Outdoors" judgment, during which half of the objects were studied once (1Enc) and the other half three times (1Enc). Subsequently, a surprise test phase was conducted during which participants observed novel foils, identical targets, and similar lure items. Targets could have been studied once or three times. Lures were similar but not identical to an item that could have been studied once or three times. Subjects were asked to judge "Same or Different," the former judgment accurately identifying targets and the latter accurately rejecting lures. (b) Mean target hit rate is increased for 3Enc targets, as is lure false alarm rate (i.e., diminished lure rejection rate) for 3Enc lures at intermediate levels of similarity (bins 2-4). Overall lure rejection rate is diminished with repetition via the area under the curve (AUC) summary value. (1Enc = singly studied items; 3Enc = triply studied items; * indicates significance at $p < 0.05$ two-tailed; error bars are mean +/- SEM.)

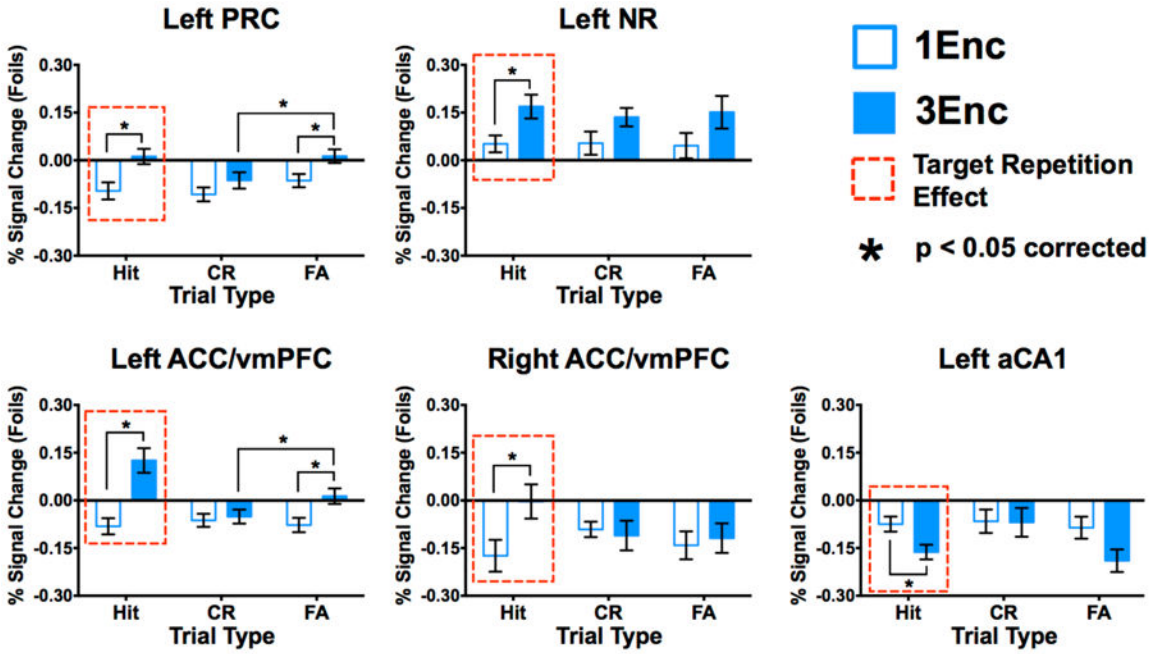

Figure 2. Repetition-related facilitation in anterior cortical regions, and suppression in anterior hippocampal CA1 during target recognition

3Enc targets elicited greater engagement than 1Enc targets in left PRC (a), left NR (b), and left ACC/vmPFC (c), and right ACC/vmPFC (d). Left anterior CA1 showed lower engagement during 3Enc targets than during 1Enc targets (e), the opposite of anterior cortices. Moreover, Left PRC (a) and ACC/vmPFC (c) showed a similar repetition enhancement for 3Enc false alarms. (1Enc = singly studied items; 3Enc = triply studied items; PRC = perirhinal cortex; NR = nucleus reuniens; ACC/vmPFC = anterior cingulate cortex/ventromedial prefrontal cortex;. * indicates significance at $p < 0.05$ corrected, two-tailed; error bars are mean +/- SEM.)

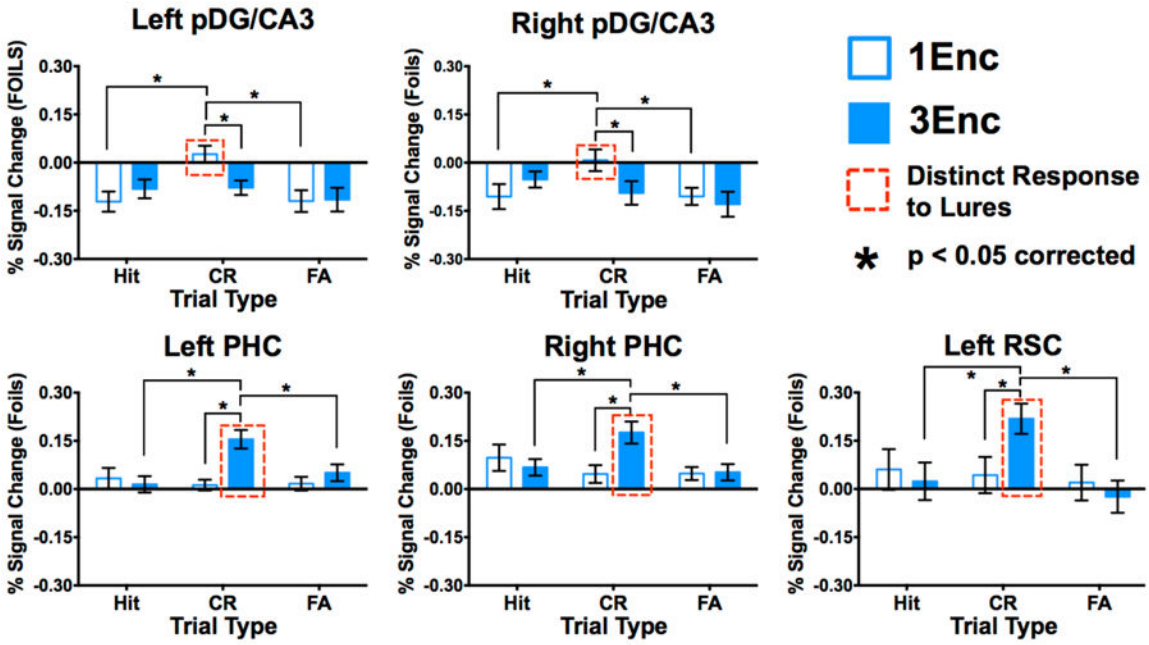

Figure 3. Repetition facilitates lure-related signals in posterior cortices, but diminishes responses in posterior DG/CA3

Unique CR > FA response pofiles for 1Enc lures were observed in both left (a) and right pDG/CA3 (b). This was not observed in these regions for 3Enc lures. Left pDG/CA3 also showed a 1Enc CR > 3Enc CR difference. Conversely, we observed CR > FA response profiles for 3Enc lures in left (c) and right PHC (d), and left RSC (e). All cortical regions showed 3Enc CR > 1Enc CR differences. (1Enc = singly studied items; 3Enc = triply studied items; CR = correct rejection; FA = false alarm; pDG/CA3 = dentate gyrus/CA3 in the posterior hippocampus; PHC = parahippocampal cortex; RSC = retrosplenial cortex; * indicates $p < 0.05$ in a Holm-Šidák post-hoc test, corrected for multiple comparisons; error bars are mean +/- SEM.)

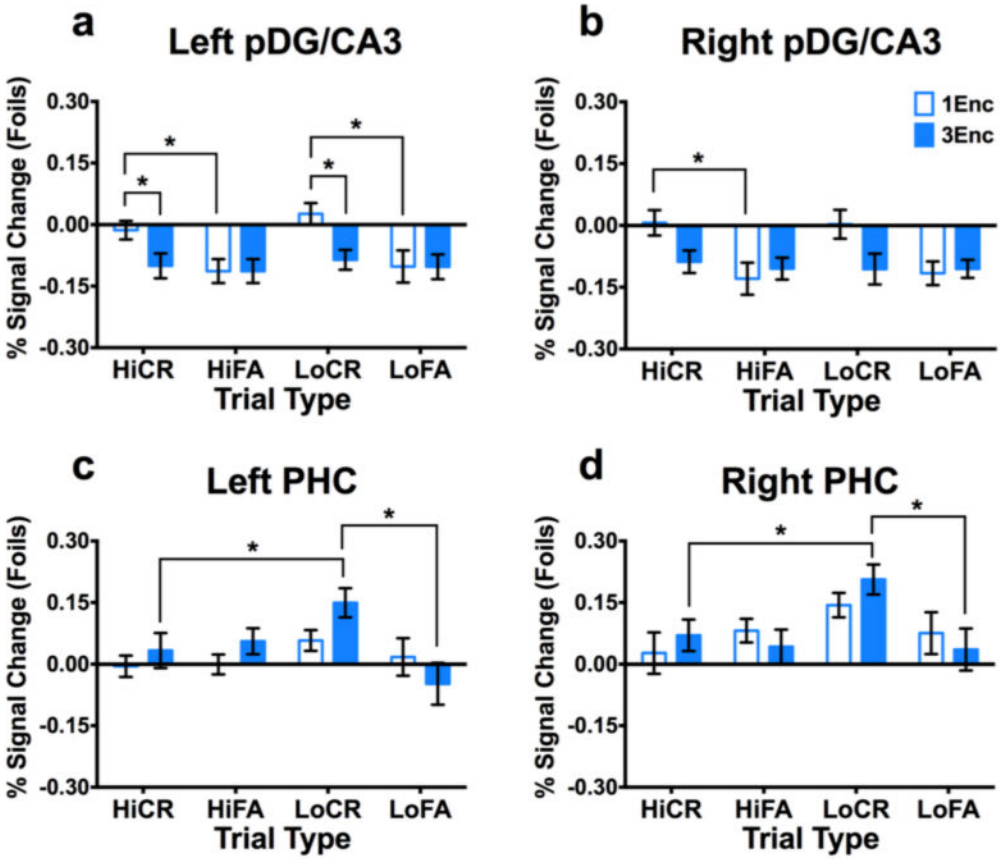

Figure 4. Posterior DG/CA3 is sensitive to high and low similarity lures, whereas PHC is sensitive only to low similarity lures

(a) Left pDG/CA3 showed greater engagement during 1Enc CRs than 1Enc FAs and 3Enc CRs across both high and low similarity levels. (b) Right pDG/CA3 showed only a significant difference between 1Enc CRs and FAs at high similarity levels, though the overall pattern is qualitatively similar to left pDG/CA3. Both left (c) and right (d) PHC showed significantly greater engagement during 3Enc CRs than FAs at low similarity levels. Moreover, engagement was greater for low similarity 3Enc CRs than high similarity 3Enc CRs. (1Enc = singly studied items; 3Enc = triply studied items; Hi = high similarity; Lo = low similarity; CR = correct rejection; FA = false alarm; pDG/CA3 = dentate gyrus/CA3 in the posterior hippocampus; PHC = parahippocampal cortex; RSC = retrosplenial cortex; * indicates $p < 0.05$ in a Holm-Šidák post-hoc test, corrected for multiple comparisons; error bars are mean +/- SEM.)

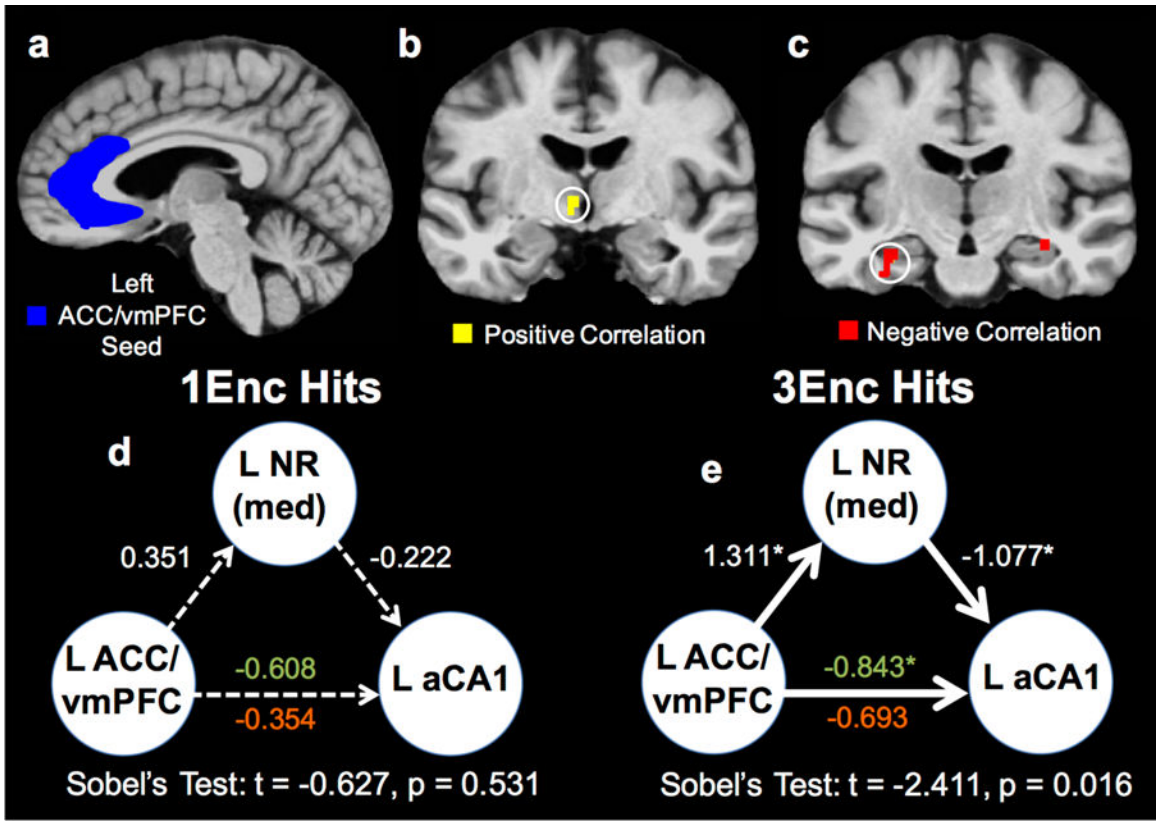

Figure 5. Anterior network functional connectivity during recognition of repeated stimuli

(a) Representative view of the left ACC/vmPFC ROI (in blue). (b) Significant positively correlated voxels from the PPI analysis (in yellow) are shown in left NR. (c) Negatively correlated voxels (in red) are shown in left (and right) aCA1. Correlation maps were thresholded via familywise error correction ($p < 0.05$, 51 contiguous voxels). (d) Mediation analyses revealed no significant connectivity for 1Enc target hits. (e) Conversely, connectivity between left ACC/vmPFC, left NR, and left aCA1 was significant during 3Enc target hits. The significant direct connectivity between left ACC/vmPFC and left aCA1 is eliminated when modeling left NR, indicating mediation is occurring to a significant degree. Critically, Sobel's test demonstrated evidence of mediation in the 3Enc condition, but not the 1Enc condition. (1Enc = singly studied items; 3Enc = triply studied items; PPI = psychophysiological interaction; NR = nucleus reuniens; ACC/vmPFC = anterior cingulate cortex/ventromedial prefrontal cortex; aCA1 = CA1 in the anterior hippocampus; green text indicates the left ACC/vmPFC to left aCA1 pathway without modeling left NR as a mediator, and red text indicates this pathway with NR mediation.)

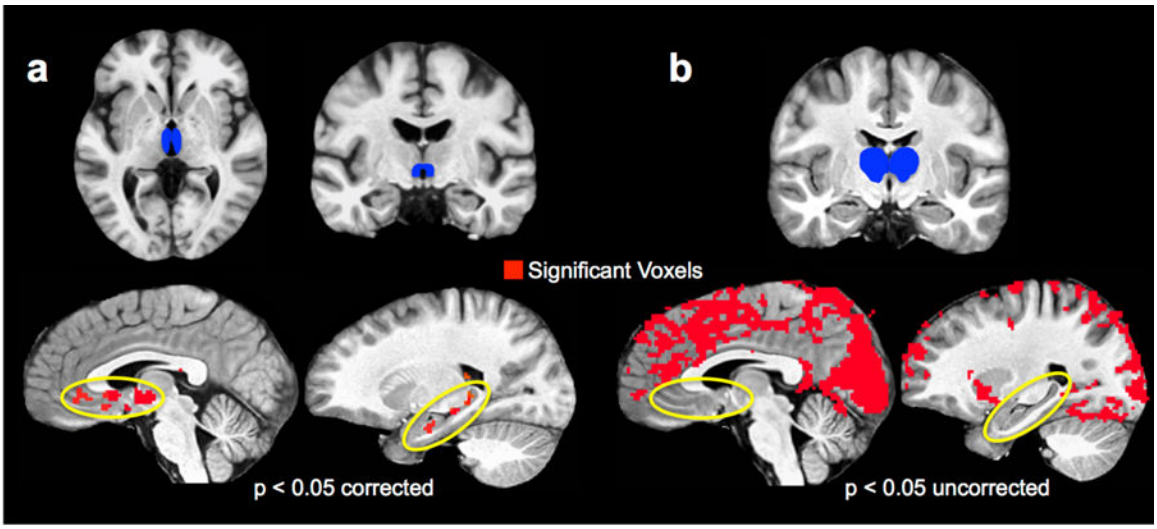

Figure 6. Resting state functional connectivity dissociates NR from the rest of the thalamus

(a) Using the NR ROI as a mask reveals significant resting state functional connectivity with the ventromedial portion of the PFC and the hippocampus along its longitudinal axis. This is displayed at a familywise error corrected threshold ($p < 0.05$ corrected, 51 contiguous voxels). (b) Using a whole thalamus ROI minus the NR ROI reveals a strikingly different connectivity pattern, with widespread connectivity excluding ventromedial PFC and the hippocampus. This is displayed at an uncorrected threshold of $p < 0.05$ to illustrate the extent to which these regions are absent. (NR = nucleus reuniens; ROI = region of interest. PFC = prefrontal cortex.)

Table 1

Main effects, interactions, and pairwise differences between conditions across significantly-modulated ROIs

Regions are organized in rows, and columns correspond to particular tests of interest. An ‘X’ is used to denote a significant effect or contrast (for contrasts with one condition ‘vs’ another, the significance threshold is corrected for multiple comparisons within a region). Note that there is high consistency across pairwise contrasts in anterior versus posterior regions, and within posterior regions, hippocampus markedly differs from adjacent cortices. (Rep = main effect of repetition; Cond = main effect of condition; Rep × Cond = interaction; 1 = singly encoded trials; 3 = triply encoded trials; CR = lure correct rejections; FA = lure false alarms.)

Region	Rep	Cond	Rep × Cond	1Hit vs 3Hit	1CR vs 3CR	1FA vs 3FA	1CR vs 1FA	3CR vs 3FA	1Hit vs 1CR	3Hit vs 3CSR
L PRC	X	X		X		X		X		X
L NR		X		X						
L ACC/vmPFC	X	X	X	X		X		X		X
R ACC/vmPFC		X	X	X						
L aCA1	X	X		X		X		X		X
L pDG/CA3		X	X		X		X		X	
R pDG/CA3			X		X		X		X	
L PHC	X	X	X		X			X		X
R PHC			X		X			X		X
L RSC	X		X		X			X		X